











# 6 Intronic Germline *DICER1* Variants in Patients With Sertoli-Leydig Cell Tumor

Claudette R. Fraire, BS<sup>1</sup> ; Paige R. Mallinger, MS<sup>2,3,4</sup>; Jessica N. Hatton, MS, CGC<sup>5</sup> ; Jung Kim, PhD<sup>5</sup> ; David S. Dickens, MD, FAAP<sup>6</sup> ; Peter A. Argenta, MD<sup>7</sup>; Samuel Milanovich, MD<sup>8</sup>; Taylor Hartshorne, BS<sup>1</sup> ; David J. Carey, PhD<sup>9</sup>; Jeremy S. Haley, MS<sup>9</sup>; Gretchen Urban, MS<sup>9</sup>; Jeon Lee, PhD<sup>10</sup> ; D. Ashley Hill, MD<sup>11</sup> ; Douglas R. Stewart, MD<sup>5</sup> ; Kris Ann P. Schultz, MD, MS<sup>2,3,4</sup> ; and Kenneth S. Chen, MD<sup>1,12</sup> 

DOI <https://doi.org/10.1200/PO.23.00189>

## ABSTRACT

Germline pathogenic loss-of-function (pLOF) variants in *DICER1* are associated with a predisposition for a variety of solid neoplasms, including pleuropulmonary blastoma and Sertoli-Leydig cell tumor (SLCT). The most common *DICER1* pLOF variants include small insertions or deletions leading to frameshifts, and base substitutions leading to nonsense codons or altered splice sites. Larger deletions and pathogenic missense variants occur less frequently. Identifying these variants can trigger surveillance algorithms with potential for early detection of *DICER1*-related cancers and cascade testing of family members. However, some patients with *DICER1*-associated tumors have no pLOF variants detected by germline or tumor testing. Here, we present two patients with SLCT whose tumor sequencing showed only a somatic missense *DICER1* RNase IIIb variant. Conventional exon-directed germline sequencing revealed no pLOF variants. Using a custom capture panel, we discovered novel intronic variants, ENST00000343455.7: c.1752+213A>G and c.1509+16A>G, that appear to interfere with normal splicing. We suggest that when no *DICER1* pLOF variants or large deletions are discovered in exonic regions despite strong clinical suspicion, intron sequencing and splicing analysis should be performed.

## ACCOMPANYING CONTENT

### Appendix

Accepted August 25, 2023

Published October 26, 2023

JCO Precis Oncol 7:e2300189

© 2023 by American Society of Clinical Oncology

Creative Commons Attribution  
Non-Commercial No Derivatives  
4.0 License

## Introduction

*DICER1*-related cancers in children and adolescents include a wide array of rare tumor types, including Sertoli-Leydig cell tumor (SLCT), pleuropulmonary blastoma (PPB), cystic nephroma, thyroid carcinoma, and pineoblastoma.<sup>1-3</sup> Most *DICER1*-related tumors are characterized by a stereotypical pattern of biallelic *DICER1* alterations. One allele exhibits a pathogenic loss-of-function (pLOF) variant, such as a nonsense, frameshift, or splice-site variant, which can be inherited in an autosomal dominant fashion or can arise de novo.<sup>2-5</sup> The other allele develops a missense variant in one of six hotspot residues in the RNase IIIa or IIIb domains of *DICER1*.<sup>2-6</sup> These are usually confined to the tumor, although individuals with somatic mosaicism for a hotspot variant can also develop multiple lung cysts and other *DICER1*-related conditions.<sup>2,7,8</sup> In particular, SLCTs are the most common type of ovarian sex-cord stromal tumor, and they tend to arise in adolescents and young adult women. Their diagnosis can sometimes be challenging, but SLCTs confirmed by central pathologic review are nearly always associated with *DICER1* variants, especially when they arise in young children or when their histology demonstrates moderate or poor differentiation.<sup>9,10</sup>

Germline pLOF variants predispose patients to development of *DICER1*-related tumors and are transmitted in an

autosomal dominant fashion.<sup>1</sup> Such variants are estimated to affect approximately 1 in 4,000 individuals.<sup>11</sup> For these patients, screening guidelines have been developed to detect tumor development early, potentially before malignant transformation or tumor progression.<sup>12</sup> Patients may also be predisposed to develop *DICER1*-related tumors when pLOF variants occur somatically in a subset of cells, such as by mosaicism. However, in a small number of patients with *DICER1*-related tumors, no pLOF variant is found in germline or tumor testing.<sup>2</sup> In these cases, it may be unclear whether to initiate surveillance for other *DICER1*-related conditions and how to counsel the family about the risk to relatives including siblings. Here, we present two cases of *DICER1*-related cancers where conventional exon-based sequencing failed to identify a pLOF variant. Using a broader sequencing panel, we identified novel intronic *DICER1* pLOF variants that lead to premature termination in both patients.

## Methods

### Institutional Review Board Approval

These studies were performed through the International PPB/*DICER1* Registry and approved by the Institutional Review Boards at Children's Minnesota, The University of Texas Southwestern Medical Center, and the Geisinger

Medical Center. Written informed consent for participation, including publication, was obtained from each participant or their guardian.

### DICER1 Sequencing Panel Design and Sequencing

DNA was isolated from blood and tumor tissue using DNeasy Blood & Tissue kit (Qiagen, Hilden, Germany). DNA was extracted from saliva using Oragene-Dx saliva collection tubes and the companion prepIT L2P kit (DNA Genotek, Ottawa, Canada). Libraries were then constructed using the NEBNext Ultra II FS DNA Library Prep Kit for Illumina (New England BioLabs, Ipswich, MA). Target enrichment was performed using the Twist Hybridization and Wash Kit with Amp Mix v2 (Twist Bioscience, South San Francisco, CA) with a custom panel of hybridization probes targeting the *DICER1* gene. Hybridization probes were designed to target a 92-kb region that includes the *DICER1* gene, with a 10-kb cushion on either side (chr14: 95076244-95168010, hg38). The custom panel contained a total of 656 probes, 120 bp each (Twist Bioscience, South San Francisco, CA). Sequencing was performed in two lanes using the MiSeq v2 micro platform (Illumina, San Diego, CA) at the UT Southwestern McDermott Next-Generation Sequencing Core. Demultiplexed reads were aligned to the reference genome (GRCh38) using BWA-MEM. Variants were called using Genome Analysis ToolKit (v3.7), Platypus, Samtools v1.4, and FreeBayes v0.9.7. Variants were then annotated using SnpEff and SnpSift (4.3r). Annotations of impact on *DICER1* were based on transcript ENST00000343455.7.

### Splicing Analysis

Tumor RNA was prepared using the miRNeasy Mini kit (Qiagen, Hilden, Germany). Reverse transcriptase PCR was performed using RT2 HT First Strand Kit (Qiagen, Hilden, Germany). RNA from the Wilms tumor cell line WiT49 was used as a wild-type control. This cell line was a gift from Sharon Plon's laboratory. PCR was performed using GoTaq G2 Flexi DNA Polymerase using the primers shown in Appendix Table A1.

Annotated variants in *DICER1* were downloaded from ClinVar on December 1, 2022. These were compared with pre-computed SpliceAI scores downloaded from Illumina BaseSpace on December 1, 2022. Those with SpliceAI scores over 0.8 are shown in Appendix Table A2.

### Biobank Cohort Analysis

UK Biobank (N = 469,787) exome (field 23157) data were used to explore two *DICER1* intronic variants, c.1509+16A>G and c.1752+213A>G. Phenotypes were evaluated using diagnosis—International Classification of Diseases (ICD)—10 (field 41270), type of cancer, ICD-10 (field 40006), ICD-9 (field 400013), underlying cause of death (field 40001), and cancer code, and self-reported (field 20001).

## Results

### Case 1

We previously reported a 2-year-old boy with thoracic SLCT<sup>13</sup> (Fig 1). His family history was strongly suspicious for an inherited pathogenic *DICER1* variant, as a paternal aunt and paternal uncle had developed tumors known to be associated with *DICER1* as children (thyroid cancer and cystic nephroma, respectively; Fig 1). *DICER1* sequencing from the proband's SLCT revealed a hotspot variant (ENST00000343455.7: c.5437G>A, p.E1813K). However, a pLOF variant was not identified by tumor sequencing, conventional germline *DICER1* sequencing including deletion testing, or chromosomal microarray. We also performed germline whole-exome sequencing and did not identify any pathogenic or likely pathogenic variants consistent with his clinical history. A variant of unknown significance in *SUFU* was also detected by clinical sequencing, although the patient and family history were not indicative of *SUFU*-associated tumors, such as basal cell carcinomas and medulloblastomas. SLCT has not previously been associated with *SUFU* abnormalities.

### Case 2

A 17-year-old girl presented with a 2-year history of amenorrhea and 2-month history of abdominal pain. Computed tomography scan showed a 17-cm septated ovarian mass. She underwent right salpingo-oophorectomy and fertility-preserving staging. She was found to have stage IA SLCT with intermediate differentiation with heterologous mucinous elements. She had no family history of *DICER1*-related cancers in immediate family or secondary relatives.

She received three cycles of cisplatin, etoposide, and bleomycin, and had no evidence of disease until 30 months after

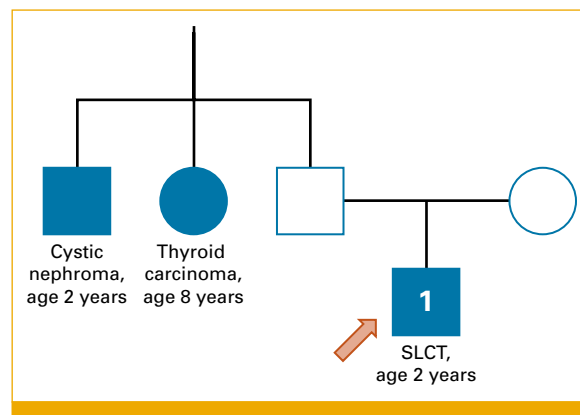


**FIG 1.** Pedigree of case 1. The proband (case 1) was diagnosed with SLCT at age 2 years. His paternal uncle and aunt, who also developed conditions that have been linked to *DICER1* variants, were tested in this study and found to have the same intronic variant. Other family members are not shown. SLCT, Sertoli-Leydig cell tumor.

completion of therapy when she presented with pain and vaginal bleeding and was found to have a left-sided ovarian mass. She underwent left salpingo-oophorectomy with pathology demonstrating poorly differentiated SLCT. She received six cycles of carboplatin and paclitaxel and had no evidence of disease until 10 months after completion of therapy when she presented with abdominal pain and was found to have a complex mass in the posterior cul-de-sac. Pathology showed SLCT. She received cisplatin, etoposide, and ifosfamide for two cycles. On the basis of molecular results and patient preference to avoid inpatient chemotherapy, she then received sorafenib, celecoxib, and oral cyclophosphamide alternating with oral etoposide, which was continued until she presented 20 months later with pelvic pain and was found to have a left pelvic mass, histologically proven to be SLCT. She received topotecan and talazoparib for 4 months before further pelvic progression, which was treated with debulking and hyperthermic intraperitoneal chemotherapy (HIPEC) with cisplatin followed by bevacizumab and talazoparib. She remains on therapy with no evidence of disease now 3 months after her HIPEC procedure. Staging studies throughout her treatment course have shown no evidence of distant metastases, although a stable 1-cm thin-walled cystic lung lesion is present, radiographically consistent with a nonprogressed PPB (type Ir).

Tumor sequencing showed a *DICER1* RNase IIIb variant p.D1709N (c.5125G>A) at 48% frequency for both the original tumor and subsequent recurrences. A *DICER1* germline variant at c.1509+16A>G was also detected in the tumor. The significance of this variant was unknown at the time, although it was noted in the molecular diagnostic report to have the potential to impair splicing. The tumor also showed variants in the *TERT* promoter c.-124C>T at 43% frequency, *ARID2* p.T1167fs (c.3498delG) at 25% frequency, and *BCOR* p.H1501fs (c.4502\_4514, delinsTGTTGT) at 51% frequency. An *ABCC4* amplification was also detected.

### *DICER1* Sequencing

To identify novel, disease-causing variants in *DICER1*, we designed a custom panel of hybridization probes targeting an approximately 92-kb region spanning 10 kb upstream and downstream of the gene, including all introns and exons (Fig 2A). We tested this capture panel on 10 samples (Fig 2B): three samples without known variants (germline DNA from case 1, tumor DNA from case 2, and germline DNA from patient R) and seven tumor samples with known *DICER1* variants (A, B, D, E, I, K, and Q). Tumor molecular testing for patient R had shown a p.E1813G hotspot variant (64% variant allele fraction) in the absence of an identifiable germline pathogenic/likely pathogenic variant or deletion. We performed next-generation sequencing on *DICER1*-enriched libraries from each sample and obtained >1,000× mean coverage across the entire region in each sample. For all 10 samples, ≥95% of bases in the targeted region were sequenced at a depth of ≥20×.

Our custom capture panel and processing pipeline successfully recapitulated all variants that were previously identified as pathogenic or likely pathogenic by ClinVar (table in Fig 2B). Specifically, we identified the stereotypical pattern of a loss-of-function variant combined with a hotspot variant in four tumor samples (patients A, B, D, and Q). In another case (patient I), commercial germline testing had not detected any pLOF variants; in the tumor, we detected the hotspot variant in 95% of reads without a pLOF variant. In two renal tumors (patients E and K), we recovered the known germline pLOF variant. In the Wilms tumor from case E, we also found a missense variant at p.R821C (c.2461C>T), a position that has recently been shown to be vital for anchoring and measuring at the 5' end of pre-microRNAs.<sup>14</sup>

### *Intronic Variants Produce Aberrant Splicing*

Sequencing from cases 1 and 2 identified no pathogenic variants using conventional filters. Thus, to identify other potential disease-causing variants, we next examined variants predicted to affect splicing using the splicing predictor algorithm SpliceAI.<sup>15</sup> Case 1 had one such *DICER1* variant, chr14:95116240T>C (c.1752+213A>G), which had not previously been observed in large genome sequencing databases (Figs 2B, 3A). We verified that his uncle and aunt carried with the same heterozygous variant by Sanger sequencing (Fig 3B). This variant is 213 nt downstream of the intron 10 splice donor, and it is predicted by SpliceAI to produce a new cryptic splice donor at the site of the variant, with a score of 0.96 (scores over 0.8 denote high confidence, Fig 3C). Transcripts mis-spliced in this manner would retain 213 nt of intronic sequence and result in an in-frame premature termination codon 18 nt into the intron.

To verify that this intronic variant affects *DICER1* splicing, we next isolated tumor RNA from case 1. We used RNA from the WiT49 cell line, which does not contain any known *DICER1* variants, as a normal control. From both RNA samples, we performed reverse-transcriptase polymerase chain reaction (RT-PCR) using primers designed to detect abnormal splicing at this site as predicted by SpliceAI. As shown in Figure 3D, two independent pairs of primers demonstrate abnormal splicing as predicted. The lower band intensity of the abnormal product could suggest lower abundance of the abnormally spliced transcript.

Case 2 also harbored an intronic variant, chr14:95117606T>C (c.1509+16A>G, Figures 2B, 4A and 4B). This variant is 16 bp downstream of the intron 9 splice donor and is predicted by SpliceAI to produce a cryptic splice donor at the site of the variant, with a score of 0.99. As with the variant above, abnormal splicing in this manner would result in retention of intronic sequence leading to an in-frame premature stop codon (Fig 4C). We again used RT-PCR to verify that this variant affects splicing in the predicted manner (Fig 4D). Again, the abnormal RT-PCR product appears less abundant.

To classify the variants found in cases 1 and 2, we applied the ClinGen *DICER1* and miRNA-Processing Gene Variant

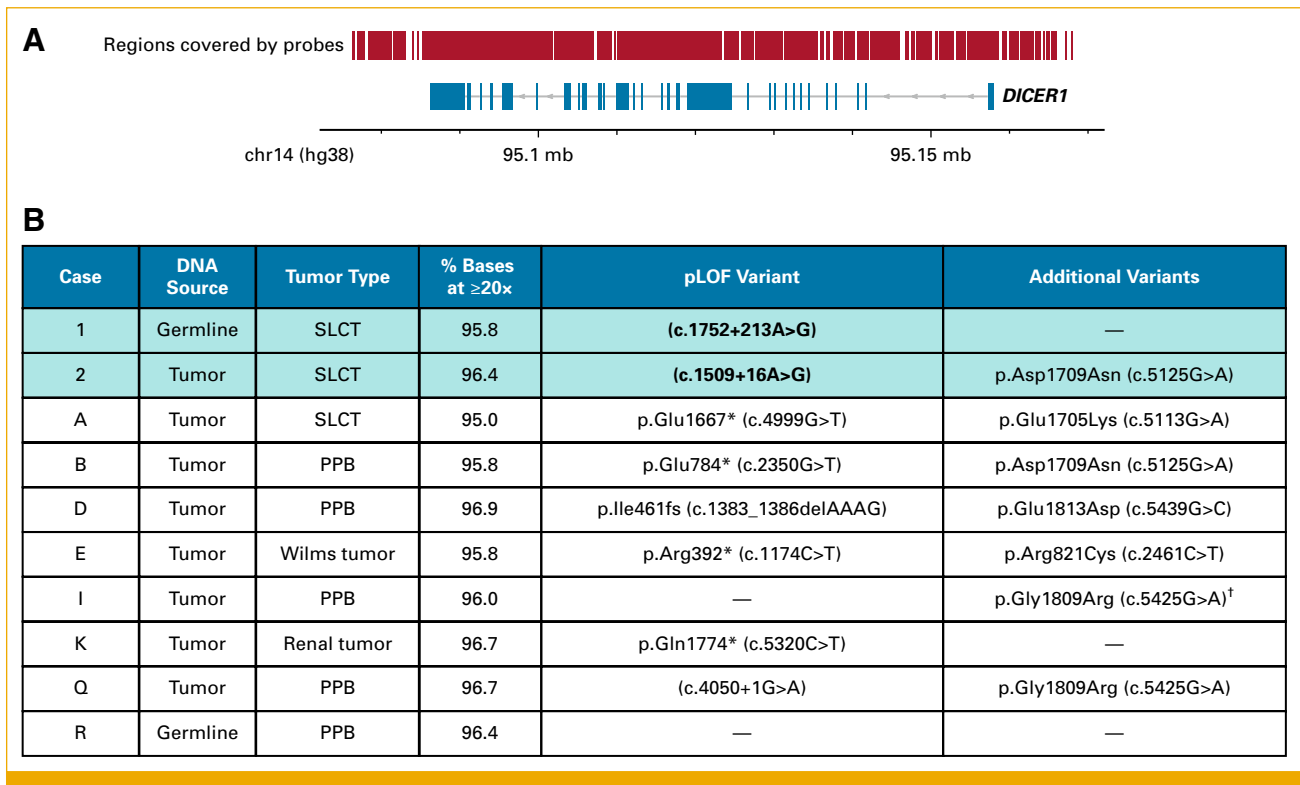


**FIG 2.** Sequencing panel. (A) Regions covered by targeted sequencing panel. (B) Metrics and results from next-generation sequencing of 10 samples, with identified pLOF and additional (hotspot) variants. In cases 1 and 2, private variants predicted to affect splicing are shown in bold. <sup>†</sup>This variant in tumor from patient I was seen in 95% of reads. pLOF, pathogenic loss-of-function; PPB, pleuropulmonary blastoma; SLCT, Sertoli-Leydig cell tumor.

Curation Expert Panel (*DICER1* VCEP) specifications to the ACMG/AMP variant interpretation guidelines<sup>16</sup> (Table 1). Since RT-PCR is not explicitly described for functional assay application in the specifications, we conservatively down-weighted this evidence as PS<sub>3</sub>\_Supporting, in line with the *DICER1* VCEP use of in vitro cleavage assays. On the basis of the clinical, segregation, tumor, functional, computational, and population evidence for the c.1752+213A>G variant in Patient C, the following evidence codes were applied, resulting in a likely pathogenic classification: PS<sub>4</sub>\_Supporting, PP<sub>1</sub>, PP<sub>4</sub>, PS<sub>3</sub>\_Supporting, PP<sub>3</sub>, and PM<sub>2</sub>\_Supporting. On the basis of the clinical, tumor, functional, computational, and population evidence for the c.1509+16A>G variant in case 2, the following evidence codes were applied, resulting in an uncertain classification one supporting criterion short of likely pathogenic: PS<sub>4</sub>\_Supporting, PP<sub>4</sub>, PS<sub>3</sub>\_Supporting, PP<sub>3</sub>, and PM<sub>2</sub>\_Supporting. Case data for both variants were shared with the *DICER1* VCEP, which relies on data sharing from various internal sources to bolster curations. This ultimately resulted in recently released likely pathogenic VCEP classifications for both variants in ClinVar (Variation IDs: 2573146, 690461) and the ClinGen Evidence Repository.<sup>17</sup>

We then explored whether these intronic variants have previously been observed in three large population cohort databases: Geisinger (170,503 exomes), UK Biobank

(469,787 exomes), and All of Us (98,560 genomes). From these three databases, we were only able to find c.1509+16A>G from one individual in UK Biobank (GQ >30, ABhet = 0.43, total read depth = 60). This individual was a male in his 60s who has never smoked with an unremarkable medical record. His only recorded ICD-10 codes found pertained to cancer screening procedures typical for patients of this age. There was no record of medication or self-reported cancer or noncancer illnesses. A second individual, in the Geisinger database, harbored a different alternate allele, c.1509+16A>C (GQ >30, ABhet = 0.36, total read depth = 28). This variant is not predicted to affect splicing. A review of this individual's medical chart includes ICD codes for hypothyroidism at age 29 years, endometrial cancer at age 37 years, and acute lymphoblastic leukemia at age 44 years. However, importantly, Geisinger and UK Biobank contain exome-sequenced data. Therefore, it is possible that a deep intronic variant such as c.1752+213A>G would have been missed.

#### Other *DICER1* Variants of Uncertain Significance May Impair Normal Splicing

Pathogenic loss-of-function variants in *DICER1* may occur through a variety of mechanisms, including the loss of normal splice sites. However, few intronic pLOF variants have been previously described. To investigate whether other



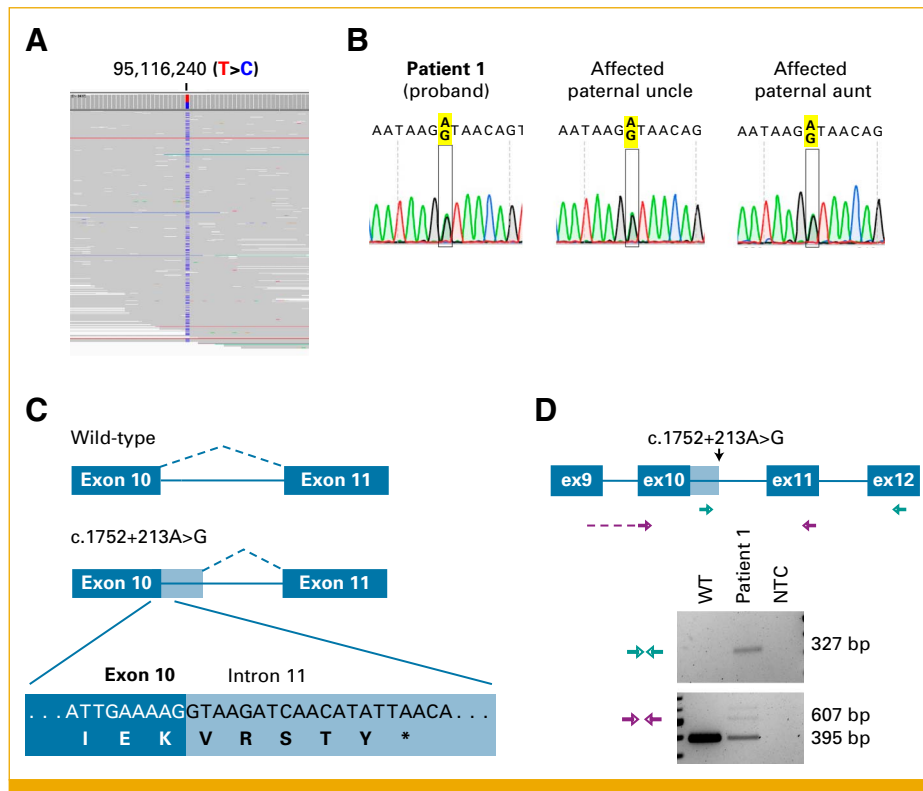


**FIG 3.** Validation of abnormal *DICER1* splicing in case 1. (A) Novel variant discovered in case 1. (B) Sanger sequencing confirming presence of variant in affected relatives. (C) The variant, ENST00000343455.7: c.1752+213A>G, is predicted to produce a novel splice donor, which results in retention of the first part of intron 10 and an in-frame premature stop codon. (D) Confirmation of the aberrant splicing product by RT-PCR. Samples on gel, from left to right: WiT49 WT cell line, tumor from case 1, and NTC. Locations of green and purple primers are designated in diagram above, and predicted sizes of products are shown on the right. The green primers are designed with a forward primer in the retained region of intron 10 and a reverse primer in exon 12, and these produce a 327-bp product when the cryptic splice donor is used. The purple forward primer bridges the exon 9-exon 10 junction, and the reverse primer resides on exon 11. Normal splicing produces a 395-bp product, and the aberrant splicing product migrates to 607 bp. A third, intermediate band appears to show a heteroduplex of these two products or an alternative splicing product. NTC, no template control; RT-PCR, reverse-transcriptase polymerase chain reaction; WT, Wilms tumor.

intronic *DICER1* pLOF variants affecting splicing may have previously been missed, we explored all reported single-nucleotide variants (SNVs) in ClinVar. Here, we defined intronic variants as any that were more than two bp from an intron-exon boundary. Of the 283 intronic SNVs, two are annotated as pathogenic or likely pathogenic. On the basis of SpliceAI predictions, eight of the remaining 281 intronic SNVs are likely to change splicing (listed in Table A2). All eight are currently annotated as VUSs in ClinVar, and all eight lay within nine bp of a splice site.

## Discussion

Here, we report the discovery of two highly suspicious germline intronic *DICER1* pLOF variants, including a deep intronic variant that segregates with the development of *DICER1*-related tumors in the family of case 1. These variants both produce cryptic splice donors that result in the

retention of intronic sequence, including a premature stop codon. In a recent review of 313 reported germline *DICER1* variants,<sup>5</sup> 32 (10%) were deemed splicing variants. Of these 32 variants, 24 were within 12 bp of a splice site. The other eight were not thought to be pathogenic; seven were seen in individuals with cancers not typically associated with *DICER1*, while the eighth individual also harbored a separate frameshift variant, suggesting the intronic variant was not causative.

Deep intronic variants have occasionally been reported in *DICER1*,<sup>18,19</sup> and intronic pLOF variants arise in other cancer predisposition genes with varying frequency.<sup>20</sup> For example, splicing variants account for 20%–37% of pathogenic variants in *NF1*.<sup>21–23</sup> In *BRCA1/2*, intron sequencing of 192 families with hereditary breast and ovarian cancer without exonic pLOF variants identified a single pathogenic deep-intronic variant.<sup>24</sup> Another study found that a deep intronic

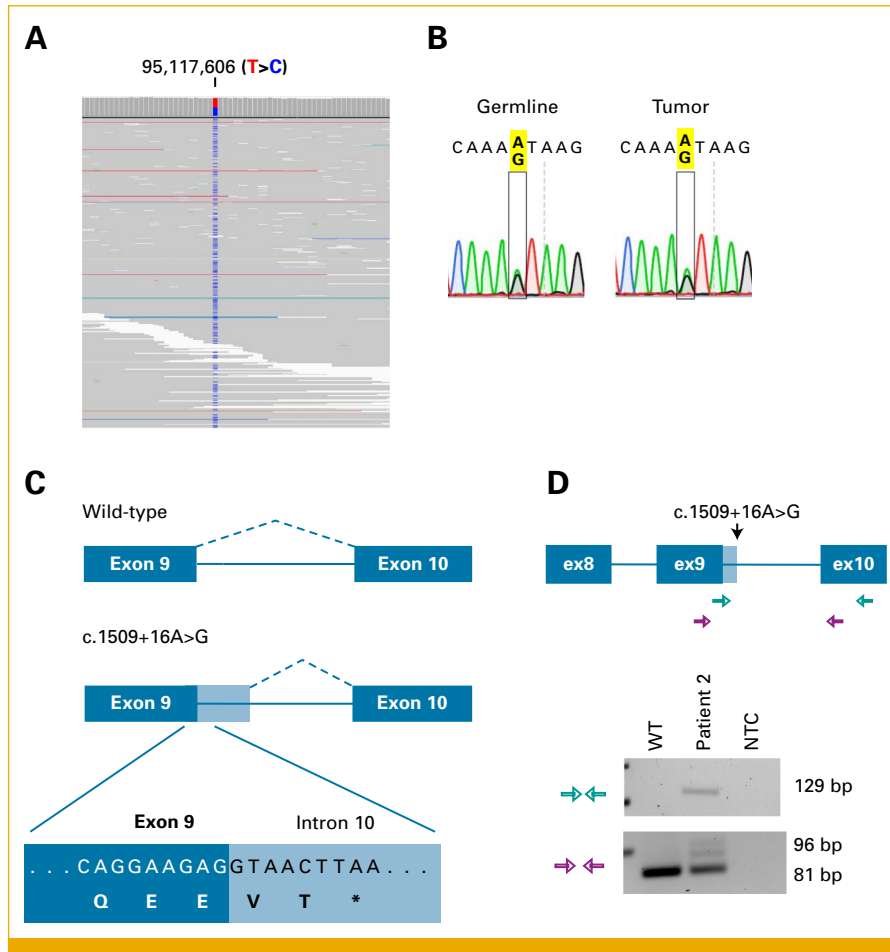


**FIG 4.** Validation of abnormal *DICER1* splicing in case 2. (A) Variant discovered in case 2. (B) Sanger sequencing confirming presence of the variant in germline and tumor DNA. (C) The variant, ENST00000343455.7: c.1509+16A>G, is predicted to produce a novel splice donor, which results in retention of the first part of intron 9 and an in-frame premature stop codon. (D) Confirmation of the aberrant splicing product by RT-PCR. The green primers sit in intron 9 and exon 10, while the purple primers sit in exons 9 and 10. NTC, no template control; RT-PCR, reverse-transcriptase polymerase chain reaction; WT, Wilms tumor.

SNV in *BRCA1*, rs191253965, which is found in <1 per 1,000 individuals in gnomAD, results in activation of a cryptic exon.<sup>25</sup> Typically, splicing defects are only considered for variants near exon-intron boundaries. However, silent exonic variants far from an intron could also affect splicing by producing a cryptic splice site or inducing exon skipping. Both effects have been demonstrated in exonic *TP53* variants.<sup>26</sup>

Clinical sequencing of cancer predisposition genes has focused on exons because of technical and analytical constraints. For instance, the sequencing panel we describe here covers approximately 9× more bases than simply sequencing the exons of *DICER1*, but advances in sequencing technology may overcome the increased cost of identifying these variants. Even when intronic variants are identified, however, interpretation of these variants remains difficult. Earlier splicing predictors were based on consensus splicing sequences, but newer prediction algorithms such as SpliceAI

use machine learning or deep learning. SpliceAI was reported to have superior sensitivity and specificity for predicting splicing changes<sup>23,27</sup> (sensitivity of 90%–95% v 69%–84% and specificity of 92%–94% v 39%–93%, for SpliceAI v earlier algorithms, respectively).

To identify variants that affect splicing, some clinical laboratories have begun using an alternative approach of paired DNA and RNA sequencing in cancer susceptibility genes.<sup>28,29</sup> In addition to sequencing exons from genomic DNA, transcripts are captured and sequenced from RNA. This approach has the advantage of quantifying splicing effects without relying on computational prediction, but it also has certain limitations. This paired approach requires specialized RNA collection tools, an optimized oligonucleotide capture pool for cDNA, and a reference set of splicing variation in healthy control patients. Furthermore, some alterations will be harder to detect with this approach. For example, variants that reduce transcript abundance could be

**TABLE 1.** ACMG/AMP Evidence Codes Applied According the ClinGen *DICER1* Variant Curation Expert Panel Modified Variant Classification Specifications for Germline Variant Curation of the *DICER1* Variants Identified in Case 1 and Case 2 (ENST00000343455.7:c.1752+213A>G and ENST00000343455.7:c.1509+16A>G)

Relevant Evidence Codes (point value) and Summary of <i>DICER1</i> VCEP Code Modification	Case 1: c.1752+213A>G	Case 2: c.1509+16A>G
PS4_Supporting (1 point): individual harboring germline variant has a highly specific phenotype for <i>DICER1</i> -related tumor predisposition as denoted by the VCEP	Paternal uncle with cystic nephroma	Proband with PPB type I <sub>r</sub> and ovarian SLCT
PS3_Supporting (1 point): in vitro cleavage assay demonstrates reduced capacity to produce 5p or 3p miRNA (moderate or strong application: patient-derived RNA assay demonstrates splicing impact)	RT-PCR data from tumor demonstrate abnormal splicing	RT-PCR data from tumor demonstrate abnormal splicing
PM2_Supporting (1 point): allele frequency <0.000005 in gnomAD (noncancer); ≥20× coverage	Absent from gnomAD	Absent from gnomAD
PP1 (1 point): variant cosegregation with disease across 3-4 meioses in ≥1 family	Three meioses in one family	NA
PP3 (1 point): MaxEntScan and SpliceAI both predict splice impact	Splice impact predicted	Splice impact predicted
PP4 (1 point): tumor testing reveals patient tumor harbors characteristic <i>DICER1</i> hotspot variant in addition to germline variant	Hotspot variant in SLCT	Hotspot variant in SLCT
Bayesian pathogenicity points	6	5
Final classification	Likely pathogenic (6-9 points)	Uncertain significance (0-5 points)

Abbreviations: ACMG/AMP, The American College of Medical Genetics and Genomics and the Association for Molecular Pathology; NA, not applicable; PPB, pleuropulmonary blastoma; RT-PCR, reverse-transcriptase polymerase chain reaction; SLCT, Sertoli-Leydig cell tumor; VCEP, Variant Curation Expert Panel.

harder to detect, whether by triggering nonsense-mediated decay or by removing segments of the promoter and first exon. In other cases, dedicated intron sequencing could still be required to detect a causative variant even after splicing impairment is detected by RNA-first sequencing. For instance, the variant in case 1 affects splicing by creating a cryptic splice donor, but the variant itself is not included in the alternatively spliced transcript. Other variants could affect the branch point or polypyrimidine regulatory regions. A future approach could combine full intron sequencing with upfront RNA sequencing to detect such variants.

Intronic pLOF variants in *DICER1* appear to be rare. Germline pLOF variants can be found in most *DICER1*-related tumors, and nearly all cases without germline pLOF can be explained by mosaicism or biallelic tumor variants. In our previous studies of *DICER1*-related tumors, germline or mosaic pLOF variants were found in 95 of 124 PPB cases (77%) and 25 of 41 SLCT cases (61%).<sup>2,9</sup> Of the cases without germline or mosaic pLOF variants, tumor-specific pLOF variants could be found in 19 of 21 cases of PPB (90%) and 12 of 12 cases of SLCT (100%) for whom tumor DNA was available. In sum, there were only two cases of either PPB or SLCT for which we could

not detect a pLOF variant when germline and tumor DNA were both available.

Nevertheless, finding such variants could have ramifications for both screening and therapeutic purposes. Identifying a causative variant allows a patient to undergo surveillance for early detection of *DICER1*-related tumors, and it allows family members to be tested and undergo genetic counseling.<sup>12</sup> Furthermore, abnormal splicing can be therapeutically targetable. Spinal muscular atrophy has been treated with the antisense oligonucleotide (ASO) nusinersen, which is designed to rescue a defect in *SMN1* by changing how *SMN2* is spliced. Similarly, the ASO milasen was designed to change how *CNL7* is mis-spliced by a novel variant discovered in a single patient.<sup>30</sup> In the liver, the ASO mipomersen treats familial hypercholesterolemia by targeting apolipoprotein B-100. ASO delivery to cancer cells or cancer precursors will be more challenging, but a recent study described ASOs designed to target variants in the cancer susceptibility gene *ATM*.<sup>31</sup> The intronic variants in *DICER1* splicing we describe here could conceptually be therapeutically targeted with an ASO that restores normal *DICER1* function. Further research will investigate genotype-phenotype correlations and potential therapeutic implications.

## AFFILIATIONS

<sup>1</sup>Department of Pediatrics, UT Southwestern Medical Center, Dallas, TX

<sup>2</sup>International Pleuropulmonary Blastoma (PPB)/*DICER1* Registry, Children's Minnesota, Minneapolis, MN

<sup>3</sup>International Ovarian and Testicular Stromal Tumor (OTST) Registry, Children's Minnesota, Minneapolis, MN

<sup>4</sup>Cancer and Blood Disorders, Children's Minnesota, Minneapolis, MN

<sup>5</sup>Division of Cancer Epidemiology and Genetics, National Cancer Institute, National Institutes of Health, Rockville, MD

<sup>6</sup>Department of Pediatrics, University of Iowa, Iowa City, IA

<sup>7</sup>Department of Obstetrics, Gynecology and Women's Health, University of Minnesota, Minneapolis, MN

<sup>8</sup>Pediatric Hematology and Oncology, Sanford Roger Maris Cancer Center, Fargo, ND

<sup>9</sup>Department of Genomic Health, Geisinger Clinic, Danville, PA

<sup>10</sup>Lyda Hill Department of Bioinformatics, UT Southwestern Medical Center, Dallas, TX

<sup>11</sup>Department of Pathology and Immunology, Washington University, St Louis, MO

<sup>12</sup>Children's Medical Center Research Institute, UT Southwestern Medical Center, Dallas, TX

## CORRESPONDING AUTHOR

Kenneth S. Chen, MD, UT Southwestern Medical Center, 5323 Harry Hines Blvd, Dallas, TX 75390; e-mail: kenneth.chen@utsouthwestern.edu.

## SUPPORT

Supported in part by the computational resources provided by the BioHPC supercomputing facility in the Lyda Hill Department of Bioinformatics at UT Southwestern. This work was supported by funding from the National Cancer Institute (K08CA207849 to K.S.C.; R01/R37CA244940 to K.A.S., D.A.H., and P.R.M.; and R01CA143167 to D.A.H. and K.A.S.) and Cancer Prevention and Research Institute of Texas (RR180071 to K.S.C., RP210041 to C.R.F.), as well as the Intramural Research program of the Division of Cancer Epidemiology and Genetics, National Cancer Institute, Rockville, MD.

## AUTHOR CONTRIBUTIONS

**Conception and design:** Claudette R. Fraire, Kris Ann P. Schultz, Kenneth S. Chen

**Financial support:** Kenneth S. Chen

**Administrative support:** Kenneth S. Chen

**Provision of study materials or patients:** David S. Dickens, Peter A. Argenta, Samuel Milanovich, D. Ashley Hill, Douglas R. Stewart, Kris Ann P. Schultz, Kenneth S. Chen

**Collection and assembly of data:** Claudette R. Fraire, Paige R. Mallinger, David S. Dickens, Peter A. Argenta, Samuel Milanovich, Taylor Hartshorne, David J. Carey, Jeremy S. Haley, Gretchen Urban, D. Ashley Hill, Douglas R. Stewart, Kris Ann P. Schultz, Kenneth S. Chen

**Data analysis and interpretation:** Claudette R. Fraire, Jessica N. Hatton, Jung Kim, David S. Dickens, Samuel Milanovich, Taylor Hartshorne,

David J. Carey, Jeremy S. Haley, Jeon Lee, D. Ashley Hill, Douglas R. Stewart, Kris Ann P. Schultz, Kenneth S. Chen

**Manuscript writing:** All authors

**Final approval of manuscript:** All authors

**Accountable for all aspects of the work:** All authors

## AUTHORS' DISCLOSURES OF POTENTIAL CONFLICTS OF INTEREST

The following represents disclosure information provided by authors of this manuscript. All relationships are considered compensated unless otherwise noted. Relationships are self-held unless noted.

I = Immediate Family Member, Inst = My Institution. Relationships may not relate to the subject matter of this manuscript. For more information about ASCO's conflict of interest policy, please refer to [www.asco.org/rwc](http://www.asco.org/rwc) or [ascopubs.org/po/author-center](http://ascopubs.org/po/author-center).

Open Payments is a public database containing information reported by companies about payments made to US-licensed physicians ([Open Payments](http://OpenPayments)).

**Paige R. Mallinger**

**Employment:** Children's Minnesota, Allina Health

**David S. Dickens**

**Consulting or Advisory Role:** Tempus, Inc, Amgen

**Research Funding:** Syndax (Inst)

**David J. Carey**

**Research Funding:** Regeneron

**D. Ashley Hill**

**Employment:** ResourcePath

**Leadership:** ResourcePath

**Stock and Other Ownership Interests:** ResourcePath

**Douglas R. Stewart**

**Employment:** Genome Medical

No other potential conflicts of interest were reported.

## ACKNOWLEDGMENT

The authors thank the patients and families who contributed to this study. This research has been conducted using the UK Biobank Resource under Application Number 54389. The authors thank Regeneron Genetics Center (Tarrytown, NY) for support.

## REFERENCES

1. Stewart DR, Best AF, Williams GM, et al: Neoplasm risk among individuals with a pathogenic germline variant in DICER1. *J Clin Oncol* 37:668-676, 2019
2. Brennen M, Field A, Yang J, et al: Temporal order of RNase IIIb and loss-of-function mutations during development determines phenotype in pleuropulmonary blastoma/DICER1 syndrome: A unique variant of the two-hit tumor suppression model. *F1000Res* 4:214, 2018
3. Adam MP, Mirzaa GM, Pagon RA, et al: *GeneReviews*®. Seattle, WA, University of Washington, Seattle, 1993
4. Hill DA, Ivanovich J, Priest JR, et al: DICER1 mutations in familial pleuropulmonary blastoma. *Science* 325:965, 2009
5. Kock L, Wu MK, Foulkes WD: Ten years of DICER1 mutations: Provenance, distribution, and associated phenotypes. *Hum Mutat* 40:1939-1953, 2019
6. Vedanayagam J, Chatila WK, Aksoy BA, et al: Cancer-associated mutations in DICER1 RNase IIIa and IIIb domains exert similar effects on miRNA biogenesis. *Nat Commun* 10:3682, 2019
7. de Kock L, Wang YC, Revil T, et al: High-sensitivity sequencing reveals multi-organ somatic mosaicism causing DICER1 syndrome. *J Med Genet* 53:43-52, 2016
8. Klein S, Lee H, Ghahremani S, et al: Expanding the phenotype of mutations in DICER1: Mosaic missense mutations in the RNase IIIb domain of DICER1 cause GLOW syndrome. *J Med Genet* 51:294-302, 2014
9. Schultz KAP, Harris AK, Finch M, et al: DICER1-related Sertoli-Leydig cell tumor and gynandroblastoma: Clinical and genetic findings from the International Ovarian and Testicular Stromal Tumor Registry. *Gynecol Oncol* 147:521-527, 2017
10. de Kock L, Terzic T, McCluggage WG, et al: DICER1 mutations are consistently present in moderately and poorly differentiated sertoli-leydig cell tumors. *Am J Surg Pathol* 41:1178-1187, 2017
11. Mirshahi UL, Kim J, Best AF, et al: A genome-first approach to characterize DICER1 pathogenic variant prevalence, penetrance, and phenotype. *JAMA Netw Open* 4:e210112, 2021
12. Schultz KAP, Williams GM, Kamihara J, et al: DICER1 and associated conditions: Identification of at-risk individuals and recommended surveillance strategies. *Clin Cancer Res* 24:2251-2261, 2018
13. Terry W, Carlisle EM, Mallinger P, et al: Thoracic Sertoli-Leydig cell tumor: An alternative type of pleuropulmonary blastoma associated with DICER1 variation. *Pediatr Blood Cancer* 68:e29284, 2021
14. Lee YY, Lee H, Kim H, et al: Structure of the human DICER1-pre-miRNA complex in a dicing state. *Nature* 615:331-338, 2023
15. Jaganathan K, Kyriazopoulou Panagiotopoulou S, McRae JF, et al: Predicting splicing from primary sequence with deep learning. *Cell* 176:535-548.e24, 2019
16. Hatton JN, Frone MN, Cox HC, et al: Specifications of the ACMG/AMP variant classification guidelines for germline DICER1 variant curation. *Hum Mutat* 2023:1-15, 2023
17. Evidence Repository - Clinical Genome Resources, v. 1.0.13. <https://erepo.clinicalgenome.org/evrepo/>
18. Schultz KA, Harris A, Messinger Y, et al: Ovarian tumors related to intronic mutations in DICER1: A report from the international ovarian and testicular stromal tumor registry. *Fam Cancer* 15:105-110, 2016
19. Verrier F, Dubois d'Enghien C, Gauthier-Villars M, et al: Multiple DICER1-related lesions associated with a germline deep intronic mutation. *Pediatr Blood Cancer* 65:e27005, 2018



20. Alba-Pavon P, Alana L, Astigarraga I, et al: Splicing-disrupting mutations in inherited predisposition to solid pediatric cancer. *Cancers (Basel)* 14:5967, 2022
  21. van Minkelen R, van Bever Y, Kromosoeto J, et al: A clinical and genetic overview of 18 years neurofibromatosis type 1 molecular diagnostics in the Netherlands. *Clin Genet* 85:318-327, 2014
  22. Giugliano T, Santoro C, Torella A, et al: Clinical and genetic findings in children with neurofibromatosis type 1, Legius syndrome, and other related neurocutaneous disorders. *Genes (Basel)* 10:580, 2019
  23. Ha C, Kim JW, Jang JH: Performance evaluation of SpliceAI for the prediction of splicing of NF1 variants. *Genes (Basel)* 12:1308, 2021
  24. Montalban G, Bonache S, Moles-Fernández A, et al: Screening of BRCA1/2 deep intronic regions by targeted gene sequencing identifies the first germline BRCA1 variant causing pseudoexon activation in a patient with breast/ovarian cancer. *J Med Genet* 56:63-74, 2019
  25. Anczukow O, Buisson M, Léoné M, et al: BRCA2 deep intronic mutation causing activation of a cryptic exon: Opening toward a new preventive therapeutic strategy. *Clin Cancer Res* 18:4903-4909, 2012
  26. Pinto EM, Maxwell KN, Halalsheh H, et al: Clinical and functional significance of TP53 exon 4-intron 4 splice junction variants. *Mol Cancer Res* 20:207-216, 2022
  27. Wai HA, Lord J, Lyon M, et al: Blood RNA analysis can increase clinical diagnostic rate and resolve variants of uncertain significance. *Genet Med* 22:1005-1014, 2020
  28. Landrith T, Li B, Cass AA, et al: Splicing profile by capture RNA-seq identifies pathogenic germline variants in tumor suppressor genes. *NPJ Precis Oncol* 4:4, 2020
  29. Horton C, Cass A, Conner BR, et al: Mutational and splicing landscape in a cohort of 43,000 patients tested for hereditary cancer. *NPJ Genom Med* 7:49, 2022
  30. Kim J, Hu C, Moufawad El Achkar C, et al: Patient-customized oligonucleotide therapy for a rare genetic disease. *N Engl J Med* 381:1644-1652, 2019
  31. Kim J, Woo S, de Gusmao CM, et al: A framework for individualized splice-switching oligonucleotide therapy. *Nature* 619:828-836, 2023
-

## APPENDIX

TABLE A1. Primers Used in This Study

Oligos	Sequence	Application	Size
AAAC_var73_F	TCCCTCCCAGTTCCAATCGTA	Sanger sequencing	618 bp
AAAC_var73_R	GGTTCGTTTTGATTTGCCAC	Sanger sequencing	
Di_in10 qF	ATCTCAAAAGAGGTGTACTCTGTGT	RT-PCR (AAAL)	327 bp
Di_ex12 qR	ATCAGGCAACTCTCGGGTTC	RT-PCR (AAAL)	
Di_ex9_10 qF	AGAGGTACTTAGGAAATTTGAGCA	RT-PCR (AAAL)	395 bp wildtype
Di_ex11 qR	TGTGTCCAATGGCCGTGT	RT-PCR (AAAL)	607 bp mutant
AAAN_in9 mut F	GTCCACAGATCTATGTGGTGAAGA	Sanger sequencing	600 bp
AAAN_in9 mut R	TGCAGTTGTGTAACATCAATCCAAT	Sanger sequencing	
Di_in9 qF3	CAGGAAGAGGTAACCTAAATCAA	RT-PCR (AAAN)	129 bp
Di_ex10 qR3	ATCAAACGAACCACCAAGTT	RT-PCR (AAAN)	
Di_ex9 qF2	GCCTCGCAACAAACAGATGG	RT-PCR (AAAN)	81 bp wildtype
Di_ex10 qR2	AGGTTGGTCTCATGTGCTCG	RT-PCR (AAAN)	96 bp mutant

Abbreviation: RT-PCR, reverse-transcriptase polymerase chain reaction.

TABLE A2. Intronic Single-Nucleotide Variants From ClinVar With Predicted Effects on Splicing

Name	Clinical Significance	DS_AG	DS_AL	DS_DG	DS_DL
NM_177438.3(DICER1):c.1753-9A>G	Uncertain significance	1.00	0.92	0.00	0.00
NM_177438.3(DICER1): c.3093+9T>G	Uncertain significance	0.00	0.00	0.92	0.00
NM_177438.3(DICER1): c.2256+6T>A	Uncertain significance	0.00	0.00	0.36	0.85
NM_177438.3(DICER1):c.2117-9A>G	Uncertain significance	0.98	0.38	0.00	0.00
NM_177438.3(DICER1):c.308-3T>G	Uncertain significance	0.00	0.87	0.00	0.00
NM_177438.3(DICER1): c.2256+5G>C	Uncertain significance	0.00	0.00	0.29	0.91
NM_177438.3(DICER1):c.2257-7A>G	Uncertain significance	1.00	0.75	0.00	0.00
NM_177438.3(DICER1):c.1908-3C>G	Uncertain significance	0.56	0.95	0.00	0.00